Thermoelectric harvesting for an autonomous self-powered temperature sensor in small satellites

Machin Llanos, Jorge; Bouwmeester, Jasper

Publication date
2017

Document Version
Final published version

Published in
Proceedings of the 68th International Astronautical Congress

68th International Astronautical Congress (IAC), Adelaide, Australia, 25-29 September 2017.

IAC-17,B4,6B,15,x40480

Thermoelectric harvesting for an autonomous self-powered temperature sensor in small satellites

Jorge Machin Llanos[a]*, Jasper Bouwmeester[b]

[a] *Delft University of Technology (TU Delft), The Netherlands,* J.MachinLlanos@student.tudelft.nl
[b] *Delft University of Technology (TU Delft), The Netherlands,* jasper.bouwmeester@tudelft.nl
* Corresponding Author

Abstract

There are several benefits of using autonomous sensors in spacecraft. Avoidance of wired connections reduces cost, mass, and increases the flexibility and reliability of the system. The impact of wire reduction can be significant, especially for small satellites with many sensors, like temperature and sun sensors. Previous research has already focused on wireless intra- spacecraft communications. This research tests the self-powering capabilities of a system based on a COTS thermoelectric generator connected to a Bluetooth Low Energy communication system, with a built-in controller and temperature sensor, and a power management interface. The system will be considered as a candidate for an autonomous temperature sensor in a future PocketQube mission of Delft University of Technology.

Controlled temperature differences can be achieved in a test environment, allowing the measurement of the generator power capabilities. It is tested that the system requires, for operation, a minimum temperature difference of 2.31 K between the extremes of the thermoelectric generator. It generates a peak power of 234 uW for that difference. In addition, the voltage difference obtained of 35.5 mV exceeds the minimum voltage required by the power management subsystem to be used. The power management sub-system consists of an ultra-low power converter that provides an output voltage of 4.1 V and a measured power efficiency of 32 % Moreover, thanks to the management of the Blutooth sleeping modes, with the built-in controller and several operational amplifier comparators, an average power consumption of 5 uW is required during operation. The case studied would allow measuring temperature and sending the data over a Bluetooth link to the on-board computer every 16.2 seconds

It is concluded that the technology, based on COTS components, can be implemented and considered as the first step for a fully autonomous sensor with thermoelectric power generation in small satellites. Its implementation may provide substantial advantages for remote or/and locations where wiring is difficult to integrate. The tested performance values provide the foundation to develop the technology further.

Keywords: PocketQube, Thermoelectric harvesting, wireless intra-spacecraft communication, autonomous sensor

Nomenclature

α	Seebeck coefficient (mV/K)
π	Peltier coefficient (V)
ΔT	Thermoelectric generator temperature difference (K)
b	Systematic uncertainty (-)
D	Duty cycle (%)
I_{TEG}	Current through the TEG (A)
t_{ON}	Time sensor is ON (s)
T	Sensing period (s)
T_h	Hot side temperature (K)
R_i	Internal TEG resistance (Ω)
R_L	Load resistance (Ω)
$\dot{Q}_P$	Heat produced due to Peltier effect (W)
V_{TEG}	TEG voltage produced (mV)

Acronyms/Abbreviations

BLE	Bluetooth Low Energy
COTS	Commercial off-the-shelf
GEO	Geostationary Orbit
LDO	Low dropout linear regulator
PM	Power Management
SoC	System on Chip
TEG	Thermoelectric generator
TU-Delft	Delft University of Technology

1. Introduction

Space missions benefit from the use of smaller, faster-to-develop, and cheaper spacecraft. A reduction in system size and an improvement in integration can be fulfilled with the use of self-powered autonomous sensors instead of wired sensors. Compared to batteries

they can last for longer mission times. In addition, new technology concepts, as sensors in remote or unreachable locations, can be envisioned thanks to the elimination of wires. An autonomous sensor is characterized by its wireless intra-spacecraft communication module and its self-powering module.

Several researchers have already spotted the benefits of using wireless intra-spacecraft communication [1][2][3]. The main benefits can be summarized as a reduction in mass, space, and complexity, failure isolation, and flexibility increase. Energy harvesting is related to these benefits in the same way, as it is used to eliminate harness.

Research on the self-powering field for satellites has already been carried by companies and research institutions. Analysis has already been made on the introduction of thermoelectric harvesting and radio frequency harvesting for the exterior part of a GEO broadcasting satellite. [4] [5]. A piezoelectric harvesting design has been tested to obtain energy from the micro jitter of external components of the satellite [6]. An autonomous sun sensor was designed and tested in a Cubesat mission [7]. And TEGs will be space characterized to obtain in-space performance for a future application in a mission [8].

However, no research has focused on the design and testing of a complete internal self-powered autonomous sensor for a small satellite, using COTS components. This kind of research would identify possible showstoppers and it would be used as a reference for future analysis and applications. This research characterizes the performance of the modules required on a future thermoelectrically powered autonomous sensor for small satellites. The design aims for small design volume and for the smallest operational temperature difference.

The research focuses on its possible inclusion of a proof-of-concept in the next TU-Delft mission, the Delfi-PQ, the first PocketQube mission after a long heritage in Cubesat technology [9].

This paper starts with some theory on thermoelectric energy harvesting, in Section 2, and the presentation of the envisioned and tested system, in Section 3. In section 4, the test set-ups are discussed.. Afterwards in Section 5, the results of the different characterization tests are presented. In the end, in Section 6, the conclusions and recommendations are given.

2. Thermoelectric harvesting theory

The working principle of a thermoelectric generator device is the so-called Seebeck effect, electrical power is generated when there is a temperature gradient between two in contact dissimilar conductors. The effect can be modelled as follows,

$$V_{TEG} = \alpha \Delta T \tag{1}$$

Another thermoelectric effect needed for the heat balance equation of the module is the Peltier effect. It states that when there is a voltage difference there will always be heat generated. The effect is modelled as follows,

$$\dot{Q}_P = \pi * I_{TEG} = \alpha T_h I_{TEG} \tag{2}$$

In addition, the current and the power provided to the load can be obtained with equation (1) and Ohm's law,

$$I_{TEG} = \frac{\alpha \Delta T}{R_i + R_L} R_L \tag{3}$$

$$P_{out} = VI = \frac{(\alpha \Delta T)^2}{(R_L + R_i)^2} R_L \tag{4}$$

3. Self-powered autonomous sensor design

An autonomous sensor can be self-powered as it stays in sleep mode most of the time. Therefore, its most important characteristic is its duty cycle, presented in (5).

$$D = \frac{t_{ON}}{T} = \frac{advertising\ time}{advertising\ time + charging\ time} \tag{5}$$

The active time or advertising time represents the time required for sensing, controller operations and transmitting the information. The powered subsystem has three possible roles, initialization, active mode also called advertising mode, and sleep mode. The charging time is from an advertising event until the capacitor stores enough energy for another active process.

The self-powered autonomous sensor is composed of 5 subsystems. The powering subsystem (the thermoelectric generator), the power management subsystem, the communications subsystem, the sensor, and the controller. The different modules are presented in Figure 1.

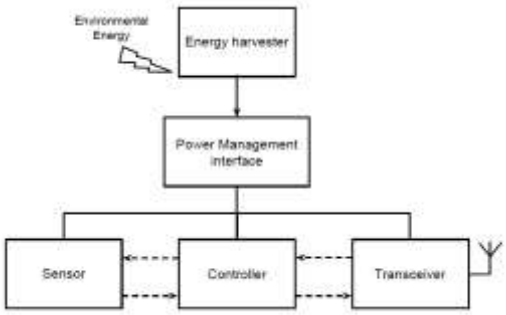

Figure 1. Sketch of the system modules.

3.1 The powering subsystem

Powering is provided by a COTS thermoelectric module. The thermoelectric module selected is the ET20,68,F1A,1313,11 from LairdTechnologies. It has been selected after a trade-off between the known-available commercial options seeking high Seebeck coefficient and low internal resistance. The TEG performance specifications are presented in Table 1.

Table 1. Specifications of the thermoelectric generator.

Specifications of TEG	Value
Internal resistance	3.55 Ω
Maximum heat generated	9.3 W
Maximum current	2.0 A
Maximum temperature gradient	67.0 K
Seebeck Coefficient	25.5 mV/K
Dimensions	13.2 x 13.2 x 2.2 mm

3.2 The communications subsystem

Previous research compared different wireless communication protocols for intra-spacecraft communication. The conclusion is that Bluetooth Low Energy has better power consumption characteristics per transmitted bit for data bus communication compared to Wi-Fi and ZigBee communication [10] . The research in this paper departs from these conclusions. Consequently, the BLE113 module is selected. It has a low average communication power and it includes a temperature sensor and a microcontroller, lowering the complexity of its integration in a system.

The method for data communication selected is the "advertising" mode of Bluetooth. In this mode, the transmitter broadcasts data to a non-specified receiver. It does not require pairing of the Bluetooth devices and the communication is only one-way. Advertising produces the lowest power consumption and the easiest implementation for data packets limited to less than 31 bytes. Its disadvantage is that one-way communication yields a less robust data link compared to communication which is checked and acknowledge for potential retransmission. The BLE module performance specifications are presented in Table 2.

Table 2. Specifications of the Bluetooth low energy module, the BLE113.

Specifications of BLE113	
TX current	18.2 mA (0 dBm)
RX current	14.3 mA
Sleep mode current	1 µA
Input voltage	2.0 – 3.3 V
Size	9.15 x 15.75 x 2.1 mm

3.3 The power management subsystem

The power management module is divided into two sections. The first section consists of a voltage step-up converter as the voltage input values required by the powered components are higher than the ones provided by the TEG. The design is based on the LTC3108 and follows the manufacturer design guidelines for the additional components needed. The full section is presented in Figure 2. The datasheet specifies that the converter design is able to generate outputs of 3.3 V with a minimum input voltage of 20 mV. Therefore, a minimum temperature difference of 2 K would be required for the voltage conversion.

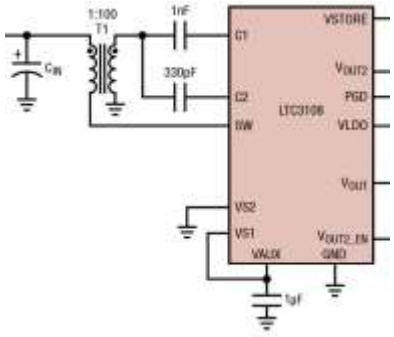

Figure 2. Recommended components connected to the LTC3108 for ultra-low input voltage levels. Image from Datasheet.

Several additional functionalities are implemented in the converter. The design uses the LDO, with an output of 2.2 V, used to provide a stable, constant, reference to the control segment of the power management subsystem.

In addition, the module requires a storage system to be able to provide energy for the power bursts. The energy used for the advertising events, peak power consumption when the sensor system should become active is provided with the energy stored in a capacitor. The capacitance used of the storage capacitor is 22 mF for testing purposes and does not represent the optimal required capacitance. The other important parameter of the output capacitor is the current leakage, as it will

increase the total charging time. The current leakage value of the capacitor corresponds with the average value found in the COTS capacitors. The specifications of the power converter and the storage component are presented in Table 3.

Table 3. Specifications of the power conversion section of the power management module, mainly considering the output capacitor and the LTC3108.

Specifications of converter	
Input resistance	5 Ω
Minimum input Voltage	20 mV
Size	30.0 x 32.0 x 6.0 mm
Power Efficiency	20% - 40 %
Capacitor current leakage	5 µA

The second section consists of a logic control system. The first requirement of this section is to provide a constant output voltage to the powered items. This is provided by a Low Drop-out linear regulator with a reduced quiescent current. The LDO contains also a switch that is activated when enough energy to complete the initialization mode is stored. Then, it should remain open, to sustain the sleep mode. This type of control is obtained with a non-inverting Schmitt trigger. The final functionality is to provide a signal for entering active mode. This is controlled with a non-inverting operational amplifier comparator. The circuit encompassing all these functions is presented in Figure 3.

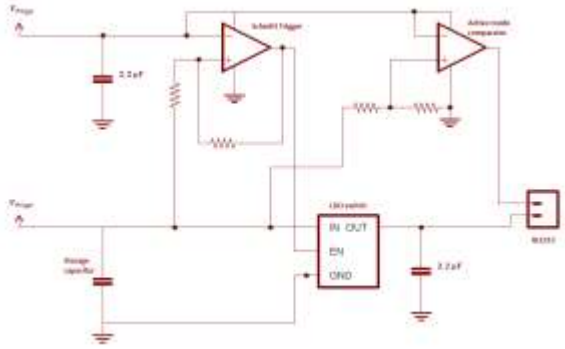

Figure 3. Circuit for the power control system.

In addition, the time diagram schematic of the system is presented in Figure 4. The initialization energy discharge is bigger than the one required for the active modes. Therefore, the Schmitt trigger should be activated before the advertising comparator because a positive signal into the BLE113 consumes enough energy to not allow to charge the storage component and so not starting with the initialization process.

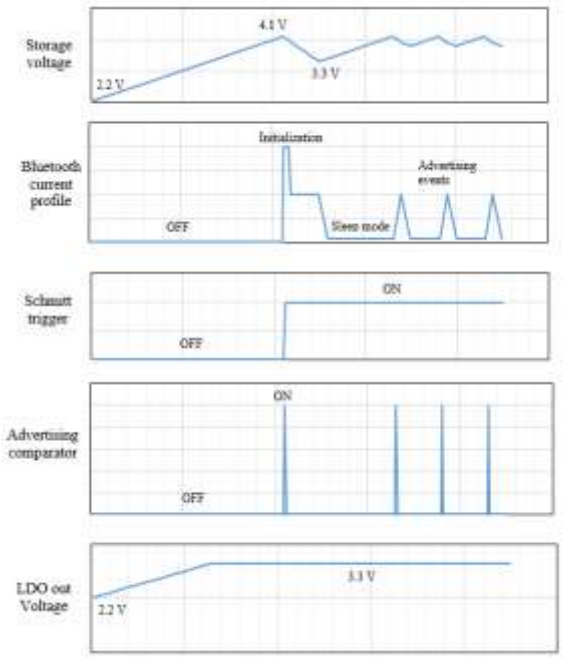

Figure 4. Time scheme of the control segment of the power management subsystem.

3.4 The controller

The BLE113 embedded controller, the CC2541, is used as the main controller of the system. This decision simplifies the system and allows easier integration than using an external controller.

3.5 The temperature sensor

The temperature sensor used is the embedded sensor in the BLE controller, the CC2541 with an accuracy of ± 2 degree after one-point calibration. It serves its purpose for a proof of concept application.

4. Test setup

The full system is tested in a modular fashion, each independent module is characterized first, before the full system connection.

4.1 Thermoelectric characterization test.

The thermoelectric generator is characterized with its IV-curve and Power curve. Power, voltage and current are measured through different load values (18Ω, 10Ω, 3.3Ω, 2Ω) for a temperature difference of 2 K. The voltage through the load is measured which allows calculating the current with Ohm's law.

Figure 5 presents a scheme of the set-up used for obtaining a known temperature gradient across the TEG. A heater is used to control the temperature difference.

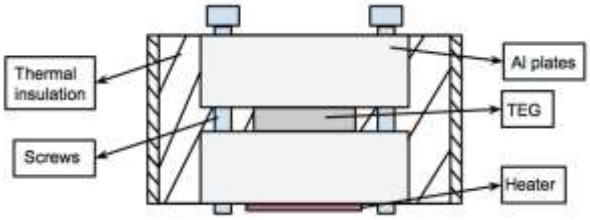

Figure 5. Thermoelectric characterization test set-up.

Thermocouples, impregnated in thermal paste, are introduced into drilled holes in both of the Al plates to measure the temperature difference. The measurement's main sources of uncertainty are presented in Table 4. They have been mitigated to guarantee successful results.

Table 4. Error sources of the measured temperatures considered as the extreme temperatures of the TEG

Elemental error sources	$b\ [T_1\ \&\ T_2]$
1. Thermometer specification	$T * 0.05\ \% + 0.5\ ºC$
2. Thermocouple standard	$1.5\ ºC$
3. Thermal contact resistance	$0.003\ ºC$
4. Spatial variation	$0.032\ ºC$

The thermal contact conductance problem is improved with the use of thermal paste between the Al plates and the module. The non-homogeneity of the thermoelectric pairs inside the module is reduced by encircling the module with a thermal insulation foam. The spatial variation of the position of the thermocouple measurement and the real position that the TEG considers in the model is considered as part of the error sources of the test

A calibration can be done to eliminate error source 1 and 2. Both thermocouples are positioned in contact with each other and the difference of temperature is determined. This difference is taken into account for corrections of the final measured values.

4.2 Bluetooth low energy characterization test

For this test, the BLE is connected through an independent power source and a shunt resistance to measure the current consumption. The shunt resistance used is equal to 15 **Ω**. Lower resistance would lower the accuracy of the measurement. Higher resistances would increase the voltage difference between the powering voltage and the input voltage seen by the BLE.

4.3 End-to-end design performance test

The main goal of this test is to obtain performance measurement for the full design. The overall performance and the proof of design is obtained with the temperature difference measurement and the power obtained in the storage capacitor that ultimately is represented by the advertising period.

The test set-up consists of the connection of the full system. The thermoelectric generator is connected to the power converter with an output capacitor of 1uF. The power converter output is then connected to the storage capacitor and its LDO output to the components specified in Figure 3.

5. Test Results and Discussion

5.1 Thermoelectric characterization results

The main aim of this test is to verify the TEG model and the product parameters, in addition to obtain a controlled and accurate testing environment for temperature differences to use in future experiments with the full system.

Figure 6 compares the model values with the measured test values. The model values are obtained with equations (3) and (4). The test values correspond to the average, data points marked with a cross, of 3 different tests. It can be seen that there is a good correlation between what is expected and what is measured.

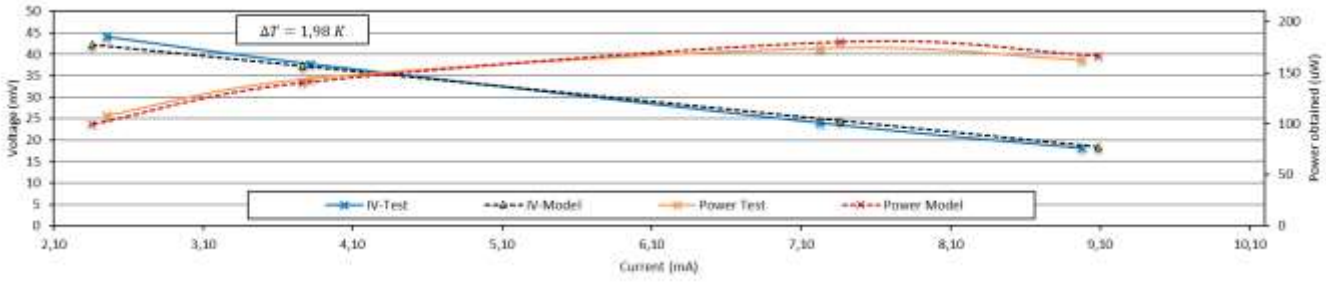

Figure 6. Thermoelectric characterization test results compared to the expected results calculated by the thermoelectric generator model.

The correlation implies that all the important error sources have been minimized

5.2 BLE characterization results

The BLE is adjusted to provide the lowest achievable power consumption. Test results have been obtained to represent the current profile by the BLE during advertising events, allowing to calculate the power consumption of the communications module to analyse what is the achievable duty cycle of the system.

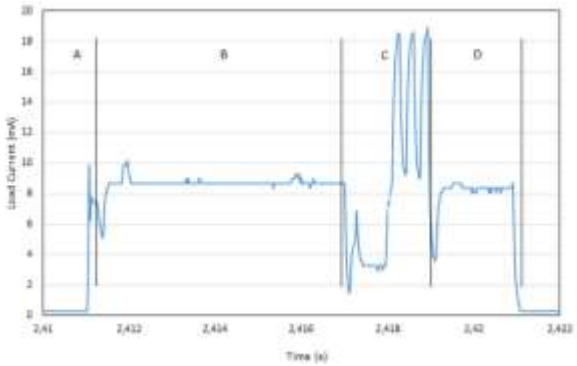

Figure 7. Current profile of the BLE113 representing a single advertising event.

The current profile for an advertising event is represented in Figure 7. Several phases can be observed in the profile. Section A represents the wake-up of the module. Section B corresponds to the temperature measurement and the stabilization of internal functions of the controller. Section C corresponds with the start of the data transmission. The three peaks correspond with the three channels used to transmit the data (Channels 37, 38 and 39). Section D represents another stabilization period embedded into the performance of the module that is required before getting into sleep mode again.

In addition, to the advertising profile, the required initialization energy needs to be measured. The current profile of the BLE module from initialization to a couple of advertising events can be seen in Figure 8.

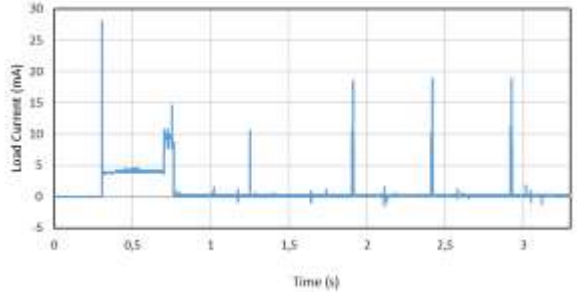

Figure 8. Current profile for the BLE module from initialization to 3 advertising events.

It can be observed that the initialization energy entails the highest amount of energy required. This initialization energy is a major design driver for the system.

Table 5. BLE113 performance values obtained in the characterization test.

BLE113 performance parameter	Value
Advertising event energy	264.4 µJ
Advertising event time	10.0 ms
Adv. Required storage capacitance	89.6 uF
Initialization energy	6.9 mJ
Initialization event time	0.4 seconds
Init. Required storage capacitance	8.2 mF

The initialization energy of the BLE113 module requires a 100 times larger capacitor, compared to a theoretical system in which initialization of the module would be ignored. It is therefore recommended for future designs to pay close attention to this power consumption and to seek for modules with as low as possible initialization energy. Nevertheless, the values obtained still guarantee the viability of the performance characterization for advertising events and the charging times of the capacitors.

This research develops a thermoelectric harvesting design based on a sensing application. However, the same design framework could be used with an actuator that scans instead of advertising as long as a certain delay in the response of the actuator is not a problem for its application. The current consumption for receiving is different than for sensing but similar values should be expected.

5.3 End-to-End design performance results

All the modules are connected. The thermoelectric generator measured powering parameters provide the operational conditions of the system. These values are presented in Table 6.

Table 6. TEG measured powering values for the End-to-end design test.

TEG input values	Value
Temperature difference	2.31 K
Input voltage	35.55 mV
Input current	6.58 mA
Peak input power	234 uW

The input current has been calculated from the input voltage and the voltage provided by the TEG due to the temperature difference measured. With these values, there is a charging in the storage capacitor. The temperature difference is not the minimum feasible but it is close to the limit of the performance. The minimum

temperature difference would increase the time required for the test to infinite, as the charging current, equal to the power converter output current minus the current losses, would be close to zero making unnecessarily long experiments. The values that are obtained from the power converter are presented in Table 7.

Table 7. Power converter performance values for the end-to-end design test.

Power Converter parameters	Value
Output current	19.24 µA
Output voltage	4.0 V
Output power	76.96 uW
Power efficiency	32 %

Ultra-low current values are obtained from the power converter module. Therefore, the use of low-leakage components is a major design driver. As an example of how much can be lost in a single component, the leakage current of the storage capacitor used equals around 25 % of the total output current obtained. The rest of the components are selected with low current leakages. The output voltage presented in Table 7 is the one in which the advertising event comparator provides a positive signal. Nevertheless, the power converter is designed for a maximum of 4.1V

The power control segment works as expected. The Schmitt Trigger first closes the LDO switch and then it remains closed. The comparator provides the signal for waking up the Bluetooth module at 4.0 V. The Schmitt Trigger should provide a positive signal slightly before the advertising comparator signal. If not, the comparator would drain energy and the initialization process won't ever be achieved. The final performance values that can be obtained from the whole system are presented in Table 8.

Table 8. Performance values obtained in the End-to-end design performance test.

System results	Value
Charging Time	16.2 seconds
Achievable duty cycle	0.06 %
Average power consumption	4.93 uW

The efficiency of the power management module is low compared to higher power DC-DC converters which typically approach 80 - 90% efficiency. If in the future the ultra-low power management modules increase their efficiencies, the duty cycle could be increased. However, this lower efficiency is obtained for obtaining a low minimum input voltage, higher input voltages would increase the requirements of the power harvesting source.

6. Conclusions

The results given in this research provide the first power values, from generator to load, for an autonomous thermoelectrically-powered temperature sensor, designed for a small satellite, for small size and temperature difference. The system design works for 2.31 K of temperature difference providing a temperature measurement over a Bluetooth Low energy (BLE) link every 16.2 seconds.

The total BLE module initialization energy required exceeded what was expected. Therefore, it is concluded that for the BLE selection, the initialization energy should be a trade-off criterion as it may drive the size of the energy storage component and consequently the size of the entire sensor system. As a recommendation, a communications module based on the SoC nRF51822 may provide better initialization values.

Table 9. Volume and mass values of the designed autonomous temperature sensor and the one used in the Delfi-n3Xt mission and connected by wires.

Parameter	Autonomous T. Sensor	T. Sensor
Height	14.4 mm	10.9 mm
Width	32.0 mm	20.0 mm
Length	30.0 mm	20.0 mm

With the technology available, it is concluded that this system does not decrease the size from a classical temperature sensor, as it can be seen in Table 9. The table presents a reference temperature sensor used in the Delfi-N3xt mission and includes a 4 pin, I2C, connector for the dimension values. The dimensions of the autonomous sensor have been optimized to not consider the conservative sizes used to facilitate testing. In addition, 2.3 mm of height of the autonomous temperature sensor could be decreased if the initialization would not drive the capacitor design. Nevertheless, the results can be used for the development of applications for remote or unreachable locations, as a sensor or an actuator. Whereas, with the current state-of-the-art technology, self-powered wireless sensors are most suitable for large satellites or where integration of the wiring harness is relatively complex, they can be carried as technology demonstrator in a PocketQube for obtaining better conclusions that will foster the implementation of the technology.

Within this study, an end-to-end development and testing campaign have proven that powering a wireless sensor with a thermal electric generator is feasible with the state-of-the-art technology and works with modest thermal gradients. Future developments are recommended to optimize the system further in terms of

size and performance and to demonstrate and characterize such systems in a real space environment.

References

[1] Amini, R., G. Aalbers, R. Hamann, W. Jongkind and P. Beethuizen. New generations of spacecraft data handling systems: Less harness, more reliability, 57th International Astronautical Congress, Valencia, Spain, 2006, 2-6 October.

[2] Amini, R., E. Gill and G. Gaydadjiev (2007). The challenges of intra-spacecraft wireless data interfacing. 58th International Astronautical Congress, Hyderabad, Andrhra Pradesh, India, 2007, 24 – 28 September.

[3] Zheng, W. H. and J. T. Armstrong "Wireless intra-spacecraft communication: the benefits and the challenges.", NASA/ESA Conference on Adaptive Hardware and Systems, Anaheim, CA, USA, 15 – 18 June 2010.

[4] Takacs, A., H. Aubert, M. Bafleur, J.-M. Dilhac, F. Courtade, S. Fredon, L. Despoisse, C. Vanhecke and G. Cluzet Energy harvesting for powering wireless sensor networks on-board geostationary broadcasting satellites. 2012 IEEE International Conference on Green Computing and Communications, Besancon, France, 20–23 Nov, 2012.

[5] Takacs, A., H. Aubert, S. Fredon, L. Despoisse and H. Blondeaux, Microwave power harvesting for satellite health monitoring. *IEEE Transactions on Microwave Theory and Techniques*, 2014, 62.4: 1090-1098.

[6] Kwon, Seong-Cheol; OH, Hyun-Ung. Experimental validation of satellite micro-jitter management strategy in energy harvesting and vibration isolation. *Sensors and Actuators A: Physical*, 2016, 249: 172-185.

[7] de Boom CW, van der Heiden N, Sandhu J, Hakkesteegt HC, Leijtens JL, Nicollet L et al. In-Orbit Experience of TNO Sun Sensors. 8th International ESA Conference on Guidance, Navigation and Control Systems. Noordwijk: ESA. 2011

[8] Von lukowicz, Marian, et al. Thermoelectric Generators on Satellites—An Approach for Waste Heat Recovery in Space. *Energies*, 2016, 9.7: 541

[9] Speretta, S., Soriano, M. T. P., Bouwmeester, M. J., Carvajal-Godinez, M. J., Menicucci, A., Watts, M. T., ... & Gill, E. Cubesats To Pocketqubes: Opportunities And Challenges. 67th International Astronautical Congress, Guadalajara, Mexico, 2016, 26-30 September.

[10] Schoemaker, R., Bouwmeester, J.Evaluation of Bluetooth Low Energy wireless internal data communication for Nanosatellites. The 4S Symposium 2014.